NIST Technical Note 1746

Accelerated Weathering of Firefighter Protective Clothing: Delineating the Impact of Thermal, Moisture, and Ultraviolet Light Exposures

Shonali Nazaré
Rick D. Davis
Jyun-Siang Peng
Joannie Chin

http://dx.doi.org/10.6028/NIST.TN.1746

National Institute of Standards and Technology
U.S. Department of Commerce

NIST Technical Note 1746

Accelerated Weathering of Firefighter Protective Clothing: Delineating the Impact of Thermal, Moisture, and Ultraviolet Light Exposures

Shonali Nazaré and Rick D. Davis
Flammability Reduction Group
Fire Research Division
Engineering Laboratory

Jyun-Siang Peng and Joannie Chin
Polymeric Materials Group
Materials and Structural Systems Division
Engineering Laboratory

http://dx.doi.org/10.6028/NIST.TN.1746

June 2012

U.S. Department of Commerce
Rebecca Blank, Acting Secretary

National Institute of Standards and Technology
Patrick D. Gallagher, Under Secretary of Commerce for Standards and Technology and Director

National Institute of Standards and Technology Technical Note 1746
Natl. Inst. Stand. Technol. Tech. Note 1746, NNN pages (June 2012)
http://dx.doi.org/10.6028/NIST.TN.1746
CODEN: NTNOEF

Abstract

Previously, the chemical and mechanical deterioration of polyaramid and polybenzimidazole-based protective clothing fabrics that resulted from concurrent thermal, moisture, and simulated sunlight exposure were quantified. This manuscript discusses the individual impacts of ultraviolet (UV) light irradiation at ambient conditions and moisture and elevated temperature in the absence of irradiation on the performance properties of outer shell (OS) fabrics used in firefighters' turnout gear. The mechanical properties which most often determine the protective performance of firefighters' turnout gear, including unidirectional stretching, tear resistance, and elastic properties, were tested before and after an accelerated weathering process. To assess and compare the protective performance of outer shell fabric samples against UV irradiation, the UV protection factor (UPF) was calculated. Attenuated Total Reflectance-Fourier Transform Infrared Spectroscopy analysis was used to elucidate the chemical changes induced by the weathering process. The data suggests that the deterioration in the physical properties of polyaramids and polybenzimidazoles are mainly due to photo-oxidative reactions, which result in chemical and mechanical deterioration of the fabrics. However, the UV exposure has a lesser detrimental effect on the UPF value.

Keywords

Accelerated weathering, UV irradiation, moisture effects, firefighters turnout gear, polyaramid, polybenzimidazole

This page left intentionally blank.

Contents

List of Tables ..... **vii**
List of Figures ..... **viii**
List of Acronyms ..... **ix**
1. Introduction **11**
2. Experimental **12**
2.1. Fabrics 12
2.2. UV aging and Thermal/Moisture aging 13
2.3. Mechanical testing 14
2.4. Ultraviolet Transmittance 15
2.5. Attenuated Total Reflection Fourier Transform Infrared Spectroscopy (ATR-FTIR) 15
3. Results and Discussion **16**
3.1. Tear Testing 16
3.2. Yarn Tensile Testing 20
3.3. UV Protection Factor (UPF) 24
3.4. Attenuated Total Reflectance Fourier Transform Infrared (ATR-FTIR) Spectroscopy 27
4. Summary and Conclusions **29**
5. References **30**

List of Tables

Table 1. Standard table for equivalance solar spectral irradiance.[10] 14
Table 2. Tear strength and loss of tear strength of NKB and KPB fabrics exposed to varying environmental conditions. Uncertainties are reported as with experimental standard deviations. 17
Table 3. Tensile strength and % elongation at break for NKB and KPB yarns exposed to varying environmental conditions. 22
Table 4. Ultraviolet protection factor (UPF) and the average UV transmittance of NKB and KPB fabrics. 25
Table 5: UPF classification system for textile materials [23] 26

List of Figures

Figure 1. Deterioration in tear strength as a function of exposure conditions for (a) NKB and (b) KPB fabrics. Error bars show experimental standard deviations. 19
Figure 2. Percent change in tear strength of UV exposed NKB and KPB fabrics w.r.t. unexposed samples.....20
Figure 3. Deterioration in tensile strength as a function of exposure conditions for (a) NKB and (b) KPB fabrics. 24
Figure 4. UPF rating as a function of UV irradiation for: (a) NKB and (b) KPB fabrics. 27
Figure 5. ATR-FTIR spectra of NKB: (a) 3550 cm^{-1} to 2950 cm^{-1} and (b) 1825 cm^{-1} to 1625 cm^{-1} stacked as a functional of aging time. Dash lines are aging at UV/50 ^{o}C/50 % RH, and solid lines at UV/25 ^{o}C/0 % RH, and dotted lines at no UV 50 ^{o}C/50 % RH. 28
Figure 6. ATR-FTIR spectra of KPB: (a) 3550 cm^{-1} to 2950 cm^{-1} and (b) 1825 cm^{-1} to 1625 cm^{-1} stacked as a function of aging time. Dashed lines represent samples aged at UV/50 ^{o}C/50 % RH, solid lines samples aged at UV/25 ^{o}C/0 % RH, and dotted lines samples aged with no UV 50 ^{o}C/50 % RH.....28

List of Acronyms

AATCC	American Association of Textile Chemists and Colorist
ASTM	ASTM International
ATR-FTIR	Attenuated Total Reflectance – Fourier Transform Infrared Spectroscopy
APP	Ageing Performance Profile
CS	Continuous Sun exposure
DMTA	Dynamic Mechanical-Thermal Analyzer
KPB	Kevlar Polybenzimidazole Blend
LOI	Limiting oxygen index
LSCM	Laser Scanning Confocal Microscopy
MCT	Mercury Cadmium Telluride
MB	Moisture Barrier
NC	Natural Conditions exposure
NFPA	National Fire Protection Association
NIST	National Institute of Standards and Technology
NKB	Nomex Kevlar Blend
OS	Outer Shell
RH	Relative Humidity
SPHERE	Simulated Photodegradation *via* High Energy Radiant Exposure
TGC	Turnout Gear Conditions
TL	Thermal Liner
UPF	Ultraviolet Protection Factor
UV	Ultraviolet
UVR	Ultraviolet Radiation Irradiance

This page left intentionally blank.

1. Introduction

Firefighter protective clothing (FFPC) is constructed of high performance fiber-containing fabrics capable of protecting against a wide range of potentially extreme exposure conditions (e.g., climate, nature and frequency of fires, firefighter's physiology, and cleaning frequency). Depending on the position of a firefighter in relation to the fire front line and type of activity in which the firefighter is involved, the firefighters' turnout gear is exposed to different conditions. The type of activity defines the thermal exposure conditions, exposure to ultraviolet (UV) radiation, level of usage, and frequency of cleaning of a turnout gear over its lifetime. The useful lifetime of turnout gear for firefighters is therefore difficult to estimate. Generally after 10 years, the FFPC is removed from service as it no longer complies with the qualitative performance metrics defined in National Fire Protection Association (NFPA) 1851 *Standard on Selection, Care, and Maintenance of Protective Ensembles for Structural Fire Fighting and Proximity Fire Fighting* [1]. The guidelines for the retirement of turnout gear however, are very limited.

The NFPA 1851 standard on selection, care, and maintenance of protective ensembles recommends retirement of the protective ensemble based on simple visual inspection and economic analysis. However, some form of degradation might not be visually detectable, for example, loss in tear strength or thermal protective performance of the ensemble due to prolonged usage and/or storage. Moreover, firefighter turnout gear is very expensive and disposal of such garments based solely on qualitative visual judgments could put undue financial burden on fire departments. It is therefore important to develop improved guidelines for the retirement of firefighters turnout gear that are based on performance metrics.

Sunlight is generally considered to be the most important element in weathering [2]. The near-UV light reaching the earth's surface delivers more energy per photon than does visible or infrared irradiation. The energies of photons in the near-UV region correspond to or exceed the covalent-bond energies of some chemical structures and therefore some bond rupture is likely to result from their absorption. Sunlight interacts with virtually all organic polymers to cause irreversible chemical changes and the photo-oxidative degradation of polymers usually leads to embrittlement, followed by loss of tensile properties. Two conditions are necessary for light of a particular wavelength to cause polymer degradation. First, the polymer must absorb the light. Second, sufficient energy must be present to break the chemical bonds. The chemical aging of the polymers often involves three main reactions: chain scission, cross-linking, and depolymerization of which chain scission largely dominates the aging process [3]. The likelihood of a given polymer to undergo chain scission depends on the nature of its constitutive chemical bonds and their particular dissociation energy. Chain scission is often coupled with oxidation, which leads to a self-sustained process that involves highly reactive free radicals produced during oxidation. The decrease in molecular weight associated with chain scission is expected to have an effect on the ultimate mechanical properties of the polymer, such as breaking strength, ultimate elongation, etc.

The mechanical properties important to the protective performance of firefighter turnout gear include unidirectional stretching, tear resistance, and elastic properties. Loss in aforementioned properties of the turnout gear fabric could result in inadequate protection and

thereby unwarranted injuries to the firefighters. Previous research [4,5,6,7,8] has established that, due to their complex physics and chemistry, high-performance fibers, in particular, are inherent absorbers of UV and undergo degradation via photolytic degradations initiated by primary photoreactions that cause main chain bond breakage. Susceptibility to photo-oxidation is particularly severe in the case of polyaramids. Photodegradation of fabrics is also related to the effects of surface treatment and abrasion damage during the weaving process. The weaving process includes application of a surface finish to the yarns and a further poly(vinyl alcohol) size application to the warp yarns. Studies [9] have shown that the surface finish may sensitize photolytic degradation of warp yarns.

In an attempt to quantify the relationship between turnout gear performance with environmental exposure, environmental stress factors were selected based on routine firefighter activities and general storage practices for turnout gear. Environmental stress factors that affect the durability of turnout gear include thermal exposure, UV radiation, moisture exposure, abrasion, and laundering. In the first phase of this work, accelerated weathering of polyaramid and polybenzimidazole outer shell (OS) fabrics was studied and reported [10]. OS fabrics were exposed to simulated UV sunlight at 50 °C and 50 % relative humidity (RH). The ageing performance profile (APP), which is the deterioration of properties as a function of time, suggested that 13 days continuous exposure (equating to 6.6 years of turnout gear exposure to UV radiation under natural conditions of usage) to the conditions mentioned above caused significant deterioration in the mechanical performance of OS fabrics. OS fabrics containing polybenzimidazole fiber blends showed less deterioration in tear resistance and tensile strength as compared to fabrics made from polyaramid fiber blends. Microscopic studies and infrared spectroscopy indicated that these exposure conditions caused significant surface decomposition of polyaramid fibers via photo oxidation while polybenzimidazole fibers showed negligible degradation. The impact of increased temperature, moisture, and UV irradiation was not singled-out during this phase of the study.

Reported here is a study of the individual environmental stress factors on the performance metrics of OS fabrics used in firefighters turnout gear, i.e. UV exposure under dry conditions and elevated moisture and temperature exposure in the absence of UV. The OS fabrics were exposed to; i) UV radiation (295 cm^{-1} to 495 cm^{-1}) at ambient temperature and 0 % relative humidity (RH) (UV /25 °C/ 0 % RH) and ii) elevated temperature and relative humidity in a 'dark' chamber with no UV radiation (no UV/50 °C/ 50 % RH). After exposure, the mechanical and chemical properties of the OS fabrics were evaluated and their APP values were compared.

2. Experimental

2.1. Fabrics

The two OS fabrics and fabric lots previously studied were used again for this study [10]. KPB is a rip-stop weave fabric constructed of a (40/60) number fraction % fiber blend of polybenzimidazole (PBI) and poly(*p*-phenylene terephthalamide) (PPA). PBI fibers have excellent heat resistance (e.g., Limiting oxygen index (LOI) of 41 %, no melting, and high

temperature strength retention) and good mechanical properties (e.g., tenacity of 2 g/denier to 3g/denier). The PPA fibers have high tenacity (22 g/denier to 26 g/denier), tensile modulus (460 g/denier to 1100 g/denier), and heat resistance (LOI of 25 % to 28 %), and very low elongation at break for tensile failure (<5 %). NKB is a plain weave fabric constructed of (93/5/2) number fraction % fiber blend of poly(*m*-phenylene isophthalate) (PPI), poly(*p*-phenylene terephthalamide), and P-140 (antistatic fiber). The P-140 fiber has a conductive carbon black core covered in a protective polyamide sheath. PPA and PPI are both polyaramids with the only chemical structure difference being the para- versus meta- linkage, respectively, in the polymer backbone. However, this difference strongly influences properties and processability of these polyaramids. PPI fibers are also inherently fire resistant fibers (LOI of 30 %) and have excellent mechanical strength (tenacity of 4 g/denier to 7g/denier and tensile elongation at break of 20 % to 30 %). Both fabrics are coated with a water-repellant coating. There are several OS manufacturers that produce similar fiber blend ratios as the fabrics used in this study, as this particular fiber blend is a very cost-effective approach to produce turnout gear complying with NFPA 1971 [11] specifications.

2.2. UV aging and Thermal/Moisture aging

In an attempt to delineate the impact of UV irradiation from heat and moisture on deterioration rate of OS fabrics, the fabrics were exposed to UV radiation at ambient temperature (25 °C ± 0.1 °C) and RH of 0 %. The fabrics were also exposed to elevated temperature and moisture conditions in the absence of UV radiation (no UV, temperature and RH of 50 °C ± 0.1 °C and 50 % ± 1 %, respectively).

UV irradiation experiments were conducted as previously described [10]. Fabric specimens with approximate dimensions of 10.2 cm × 7.5 cm (4 in × 3 in), were exposed to high UV irradiance in the NIST integrating sphere-based weathering device, referred to as SPHERE (Simulated Photodegradation *via* High Energy Radiant Exposure). Accelerated exposure of the fabrics to high UV irradiance was carried out using the mercury arc lamp system that produced a collimated and highly uniform UV flux in the environmental chambers of the SPHERE. A borosilicate glass window was placed between the lamp system and the integrating sphere to eliminate all UV wavelengths < 290 nm. The dichroic reflector in the lamps removed wavelengths > 450 nm. Additional details on the construction and properties of the SPHERE have been published elsewhere [12]. The fabric samples were exposed to UV irradiance dosage of 15.9 kJ/m^2 ± 0.02 kJ/m^2 for 24 h of the day. Based on this prescribed amount of UV exposure on the SPHERE, various parameters including continuous sun (CS) days (calculated number of days where sunlight is assumed for 24 h of the day), natural conditions (NC) day calculated assuming 9 h of sunlight in a day and exposure period for turnout gear have been calculated and reported elsewhere [10] and reproduced in Table 1.

Table 1. Standard table for equivalance solar spectral irradiance.[10]

SPEHRE (d)	Continuous Sun (d)	Natural Conditions (d)	Turnout Gear Conditions (d)	(year)
S	CS = 7.4 x S	NC = 19.7 x S	TGC = 177.3 x S	
13	96	256	2305	6.3
28	207	552	4964	13.6
42	311	827	7447	20.0
56	414	1103	9929	27.2
66	488	1300	11702	32.0

The thermal/moisture aging was conducted in experimental chambers with the same design and operational specifications as those on the SPHERE. The only difference is the 'dark side' chambers are not attached to the SPHERE.

2.3. Mechanical testing

NFPA 1971 [11] requires testing tear resistance of OS fabrics using the test procedure described in ASTM D 5587 [13]. The standard describes measurement of tear strength by the trapezoidal method (an in-the-plane tear propagation). In the textile industry, this method is not frequently used as the stress pattern measured by this method is largely determined by variables at the disposition of the operator and the tear strength values are high since the fabric yarn is pulled, not torn, apart. For these reasons, the fabric tear resistance for this study was determined using the static, single tear method described in ASTM D 2261[14]. The single tear test (also called the single rip tear test) is an out-of-the-plane tear that propagates at relatively low loads and results in tearing of the yarn and, therefore, lower tear strength values.

The single tear tests were conducted on an Instron universal testing machine (model 5582, Instron corp., Northwood, MA[1]) equipped with 2 kN load cell and custom grips for fabrics. The gauge length between grips was 25 mm, and crosshead speed was 50 mm/sec. A single 25 mm (1 in) tear was introduced at one end of specimen having approximate dimensions of 68 mm × 25 mm (2.7 in × 1.0 in). Four replicates of each fabric were tested per sampling interval. Uncertainties in measurement of tear strength are reported as Type A uncertainties [15,16] with experimental standard deviations in Table 2.

Due to specimen size restrictions, the tensile strength of the fabrics were based on yarn tensile strength values. Tensile strength or breaking strength of a fabric is generally greater than its tear strength. In the single tear test described above, each cross-section of yarn is subjected to progressively increasing tension. The cross-yarn fails singly, doubly or even in multiples,

[1] Certain commercial equipment, instruments or materials are identified in this paper in order to specify the experimental procedure adequately. Such identification is not intended to imply recommendation or endorsement by the National Institute of Standards and Technology, nor is it intended to imply that the materials or equipment identified are necessarily the best available for this purpose.

depending on the type of weave, yarn strength and elongation properties. It is important to note that in a tear test, the yarn fails individually in tension and for this reason the fabric tear strength is much lower than its breaking strength; where all yarns fail at the same time. Thus, for a more precise understanding of fabric deterioration, the individual yarns unraveled from fabrics exposed to various conditions have been tested for their tensile strength and percentage elongation properties. The yarn strength is the stress at which the yarn fails or fractures. Elongation at break is the increase in length produced by the breaking force, expressed as a percentage of the original nominal length. Since the properties depend on the specimen dimensions and testing conditions (e.g., strain rate and gauge length) the values reported here are best used for relative comparison and as absolute values to compare with results reported elsewhere.

Yarn tensile testing was measured following ASTM D2256 [17] straight strength method. Tensile properties of ply-twisted yarn from fabric specimens were measured using a TA Instruments RSA III Dynamic Mechanical-Thermal Analyzer operating in transient mode (DMTA, TA Instruments-Waters LLC, New Castle, DE). Gauge length was 10 mm and specimen extension rate was 0.005 mm/s. Since the instrument is not equipped with an extensometer, the strain was calculated by the change in grip spacing. Therefore, the data represent trends and not absolute values. A minimum of five individual ply-twisted yarns was analyzed per sampling interval. Uncertainties in measurement of tensile strength are reported as Type A uncertainties [15,16] with experimental standard deviations in Table 3. The yarn diameter was measured using an optical microscope.

2.4. Ultraviolet Transmittance

The amount of UV irradiation passing through the fabric was measured on the SPHERE. The NIST SPHERE provided the UV irradiation with an output intensity of 480 W/m^2. UV-visible transmittance spectra were measured using a Hewlett Packard 8452A diode array UV-Visible spectrophotometer (HP/Agilent, Santa Clara, CA) with a custom integrating sphere collector. The distance between the integrating sphere and the fabric specimen was kept constant (20 mm) for each measurement. The UV spectra were recorded between 290 nm to 690 nm before (to record the dark current) and after the fabric specimen was mounted. Three measurements were taken per sampling interval. The calculated UV protection factor (UPF) and the average UV transmittance may be slightly shifted from the exact values due to drift of dark current. The Type B evaluation of standard uncertainty [15, 16] for UPF was ± 5 % of the value (2 σ) [18].

2.5. Attenuated Total Reflection Fourier Transform Infrared Spectroscopy (ATR-FTIR)

ATR-FTIR analysis was used to elucidate the chemical changes induced by UV irradiation. ATR-FTIR is a technique where the infrared beam penetrates only a few microns into the specimen and therefore is appropriate for the identification of structural changes on the surface of the fabrics. Infrared analysis was carried out using a Nicolet Nexus 670 FTIR (Nicolet Instrument Corp. Madison, WI) equipped with a mercury cadmium telluride (MCT) detector and a SensIR Durascope (Smiths Detection) attenuated total reflectance (ATR) accessory. Uniform pressure was applied on the fabric using the force monitor on the durascope. Dry

breathing quality air was used as the purge gas. FTIR spectra were collected at nine different locations from fabric swatch having approximate dimensions of 102 mm × 76 mm (4 in × 3 in) and 128 scans were accumulated.

Spectral analysis, including spectral baseline correction and normalizing, was carried out using a custom software program [19] developed in the Polymeric Materials Group at NIST to catalogue and analyze multiple spectra. The spectra were baseline corrected and normalized using the peak at 781 cm^{-1} for NKB, and the peak at 820 cm^{-1} for KPB. Both peaks are attributed to out-of-plane aromatic C-H bending. Type B evaluation of standard uncertainties [15, 16] associated with this measurement are typically ±1 cm^{-1} in wave number and ± 1 % in peak intensity [18].

3. Results and Discussion

3.1. Tear Testing

A typical tear test load-extension plot has a saw-tooth shape. The middle part of the load-extension curve represents 50 % of the entire tear distance. For a given sample, determining tear strength by static single tear test method (ASTM D2261) relies on determining the median of the five largest tear forces from the middle part of the load-extension curve. Tear strength of NKB and KPB fabrics for various exposure conditions are provided in Table 2 and deterioration in tear strength is plotted as a function of exposure time in Figure 1.

14 d ± 0.5 d of UV irradiation at 50 ^{o}C and 50 % RH, the tear strength of both fabrics had significantly deteriorated (87 % and 70 % decrease for NKB and KPB fabrics respectively). Further exposures up to 56 d resulted in continued deterioration of tear strength, but at a significantly slower rate. By the end of the 56 d ±0.5 d exposure the deteriorations in percent tear strength was comparable for both fabrics (95 % and 88 % for NKB and KPB, respectively). Because of the higher initial tear strength value and slower deterioration rate, KPB maintained higher tear strength throughout the exposure duration. For example, KPB had a tear strength value of 10 N ± 0.2 N at the end of 56 d ±0.5 d exposure, which was 4 times longer than the exposure time required for NKB to reach the same value.

To quantify the contributions of UV irradiation, temperature, and moisture on tear strength deterioration, the OS fabrics were exposed either to UV irradiance at ambient conditions (UV/25 ^{o}C/0 % RH) or only elevated moisture and temperature (no UV/50 ^{o}C/50 % RH). There was no statistical change in the tear strength of the fabrics after 56 d exposure at 50 ^{o}C/50 % RH with no UV irradiation. However, UV irradiation at 25 ^{o}C/0 % RH resulted in a similar deterioration profile as previously reported for UV irradiation at 50 ^{o}C and 50 % RH (initial rapid deterioration followed by much slower deterioration rate). However, the deterioration was less severe in these UV irradiation only (UV/25 ^{o}C/0 %RH) exposures suggesting there is a contribution of higher temperature and moisture on the photo degradation of fabrics. It appears that the contribution of temperature and moisture was more critical to the KPB tear strength deterioration as the tear strength values were 15 % to 20 % lower than the full exposure conditions (NKB values were only 5 % to 10 % lower).

Table 2. Tear strength and loss of tear strength of NKB and KPB fabrics exposed to varying environmental conditions. Uncertainties are reported as with experimental standard deviations.

SPHERE (d)	NKB		KPB	
	Tear strength (N)	Approximate decrease in tear strength (%)	Tear strength (N)	Approximate decrease in tear strength (%)
No UV / 50 °C / 50 % RH				
0.0	75 ± 8.0	-	81 ± 4.3	-
14.0±0.5	76 ± 7.0	0.0	74 ± 3.1	8
28.0±0.5	68 ± 2.6	1.0	74 ± 5.2	8
42.0±0.5	68 ± 4.2	0.9	81 ± 2.6	0
56.0±0.5	72 ± 6.9	0.5	81 ± 2.3	0
UV / 25 °C / 0 % RH				
0.0	75 ± 8.0	-	81 ± 4.3	-
13.5±0.5	15 ± 0.9	80	35 ± 3.0	56
27.7±0.5	11 ± 0.7	85	26 ± 0.8	68
42.0±0.5	9.8 ± 0.5	87	22 ± 0.7	72
55.8±0.5	8.4 ± 1.3	89	21 ± 1.3	74
UV / 50 °C / 50 % RH				
0.0	75 ± 8.0	-	81 ± 4.3	-
14.0±0.5	10 ± 0.3	87	24 ± 1.5	70
28.0±0.5	5.9 ± 0.7	92	16 ± 0.7	80
42.0±0.5	4.8 ± 0.6	94	13 ± 0.5	84
56.0±0.5	4.1 ± 0.1	95	10 ± 0.2	88

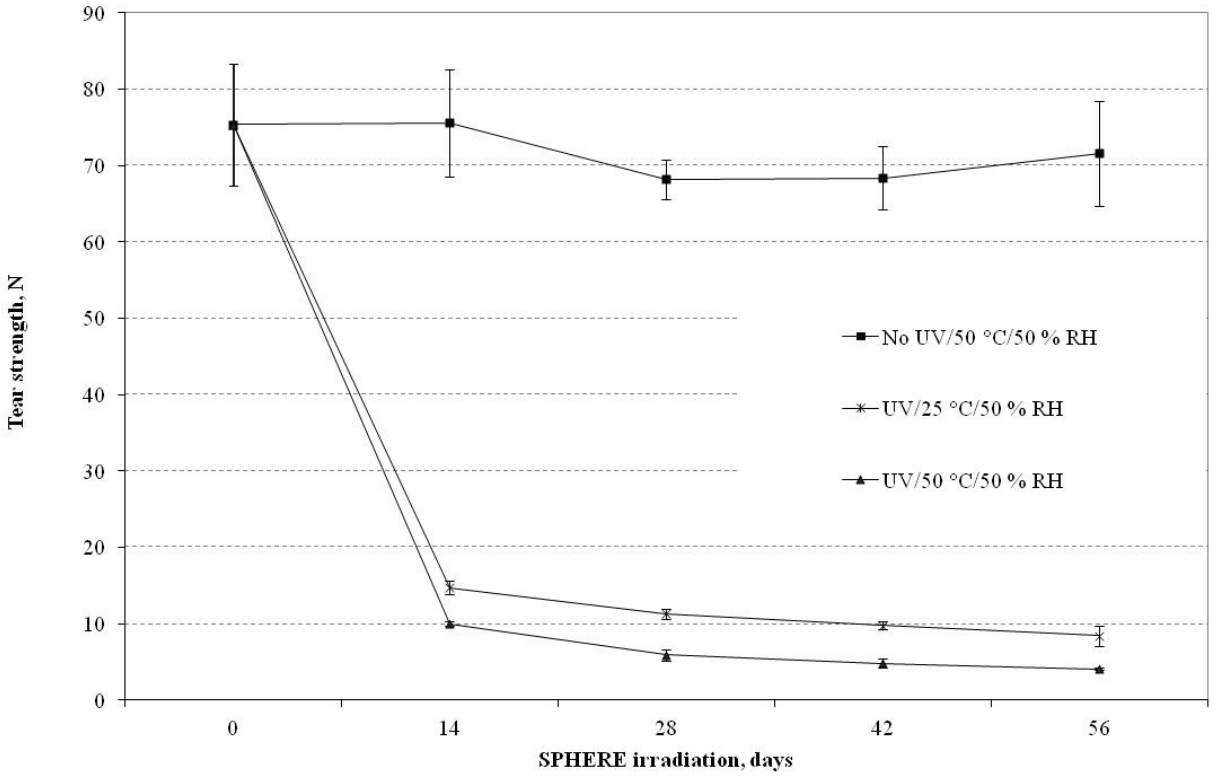
90
80
70
60
50
40
30
20
10
0
Tear strength, N
0
14
28
42
56
SPHERE irradiation, days
No UV/50 °C/50 % RH
UV/25 °C/50 % RH
UV/50 °C/50 % RH

(a)

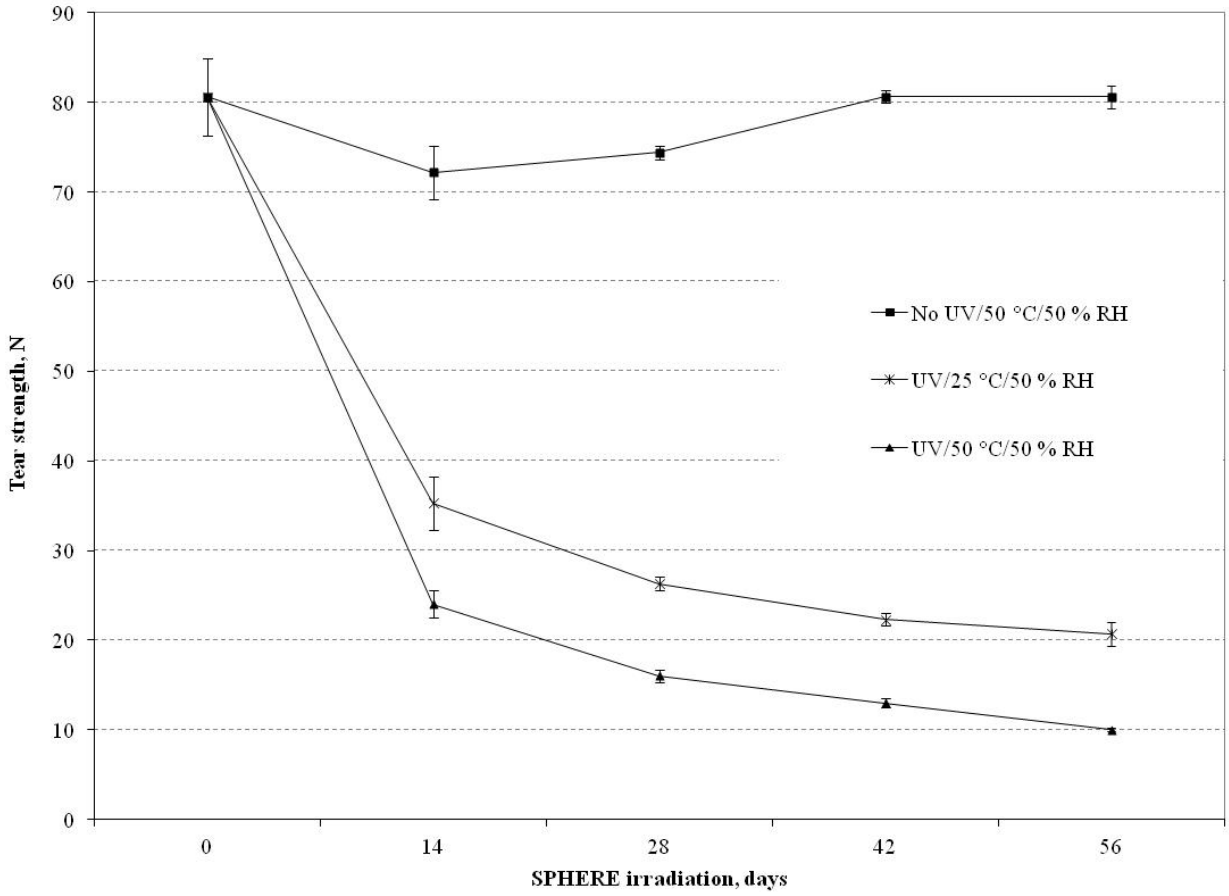

(b)

Figure 1. Deterioration in tear strength as a function of exposure conditions for (a) NKB and (b) KPB fabrics. Error bars show experimental standard deviations.

Percentage loss of tear strength with respect to unexposed control specimens for both the fabrics is plotted in Figure 2 and it can be seen that the NKB fabrics deteriorates faster than KPB fabrics suggesting that KPB has greater UV resistance. Better performance of KPB compared to NKB is due to the fact that KPB is a blend of PBI fibers and para-aramid (40/60), which both have greater UV resistance than the meta-aramid fibers used in NKB. Additionally, the meta-aramid fibers in NKB have lower tenacity (4 g/denier to 7 g/denier) than the para-aramid fibers in KPB (22 g/denier to 26 g/denier). Dobbe et al [20] have shown that para-aramids have a highly crystalline core with a less ordered skin. Any chemical degradation occurs more easily within disordered regions, which in para-aramids is only a small fraction of polymer and hence less susceptible to photo degradation. Carlsson et al [21] showed that para-aramids are more stable than meta-aramids due to increased conjugation and delocalization of absorbed energy through the enol form of the amide group in para-aramids.

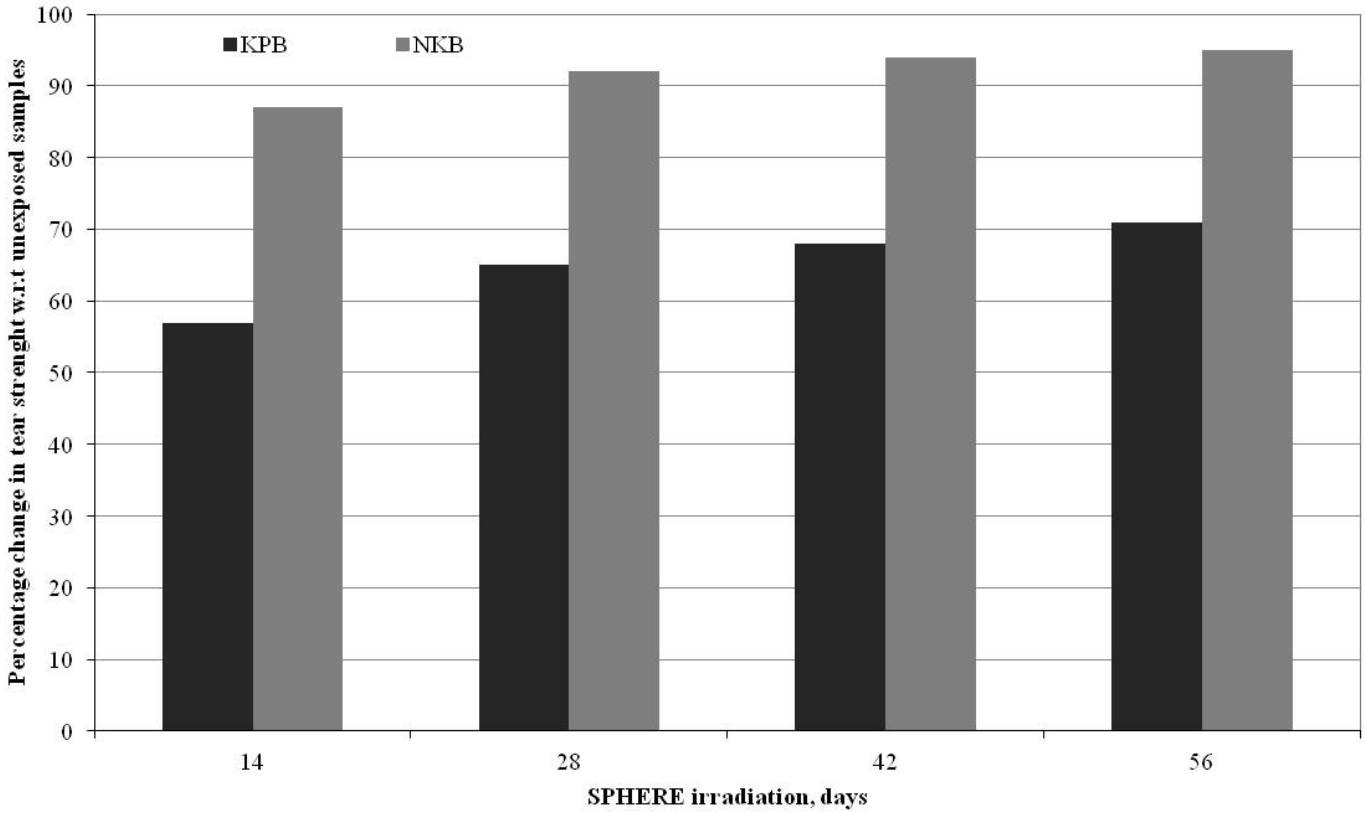

Figure 2. Percent change in tear strength of UV exposed NKB and KPB fabrics w.r.t. unexposed samples

3.2. Yarn Tensile Testing

The tensile strength and % elongation values for NKB and KPB yarns for various exposure conditions are given in Table 3 and their APP in terms of tensile strength of yarns from NKB and KPB fabrics are shown Figure 3. Stress at break was calculated based on cylindrical geometry with circular cross-section of the ply-twisted yarn. Within the uncertainties of measurements, tensile strength of unexposed NKB and KPB yarns were similar (55 ± 8 MPa). The NKB yarns exhibited ductile failure with % elongation at break of 42 % ± 7 % whereas KPB exhibited brittle failure with % elongation at break of 4.0 % ± 0.3 %. Meta-aramid fibers constitute the majority of the NKB yarns (93%) and, therefore, the NKB tensile properties were dominated by linear chain polymer fibers with inherent strength anisotropy and imperfect orientation in the fibers. This unique failure mechanism is generally contributed to the rod-like structure of liquid crystals as they are spun into fibers. The tensile failure of meta-aramid fibers is unique in that when they fail, the fibers break into small fibrils. Tensile strength failure is believed to initiate at the ends of the fibrils and is propagated through the fibers by shear. Therefore, meta-aramid fibers fail by series of fibril failures rather than a brittle failure. Such ductile failure was also confirmed by confocal microscopy in our previous studies [10].

Comparing the APP of NKB and KPB yarns in Figure 3, it can be noted that both the yarns rapidly lose tensile strength upon UV exposure. NKB yarns lost more than 80 % of their initial tensile strength after 13 d of continuous exposure to UV radiation while KPB lost only 50 % of

initial strength. Similar to loss of tear strength, further exposure up to 56 d resulted in continued deterioration of tensile strength at a significantly slower rate. The KPB yarns retained 16 % whereas NKB retained only 3 % of its original strength at the end of 56 d exposure to UV/50°C/50%RH. The UV exposure also drastically changed tensile behavior of NKB from ductile failure (% elongation at break of 41 % ± 4 %) to brittle failure (% elongation at break of 5 % ± 1.1 %). KPB yarns showed no change in failure mechanism. This is in agreement with our previous studies wherein changes in failure mechanism are illustrated by microscopic studies [10]. In absence of UV irradiation, prolonged exposures to elevated temperatures and higher moisture (no UV/50 °C /50 %RH) levels did not affect tensile properties of NKB and KPB yarns. However, in presence of UV radiation with increased temperature and moisture levels (UV/50 °C/50 %RH) there was a slightly higher deterioration in tensile strength of both NKB and KPB yarns.

Conversely, KPB yarns exhibited more brittle failure with very little elongation (4 % ± 0.3 %). Para-aramid fibers, which constitute 60 % of fibers in KBP yarns, dominate their tensile properties. Para-aramid fibers exhibit more brittle failure as compared to meta-aramid fibers. As mentioned earlier, the highly oriented structure of poly(p-phenylene terephthalamide) yields higher strength, but the fibers fail with less elongation.

Table 3. Tensile strength and % elongation at break for NKB and KPB yarns exposed to varying environmental conditions.

SPHERE (d)	NKB				KPB			
	Tensile strength (MPa)	Approximate decrease in tensile strength[§] (%)	%-Elongation	Approximate change in % elongation[^]	Tensile strength (MPa)	Approximate decrease in tensile strength[§] (%)	%-Elongation	Approximate change in % elongation[^]
No UV / 50 °C / 50 % RH								
0	55 ± 8.0	-	41 ± 4	-	55 ± 5.3	-	4 ± 0.3	-
14±0.5	56 ± 2.7	-1	41 ± 6	1	58 ± 5.8	-6	4 ± 0.5	-2
28±0.5	55 ± 4.7	0	42 ± 6	-2	58 ± 6.1	-6	4 ± 0.4	-2
42±0.5	54 ± 4.5	1	41± 4	-1	62 ± 5.3	-13	4 ± 0.4	-1
56±0.5	53 ± 4.6	4	43 ± 2	-6	61 ± 5.4	-11	4 ± 0.3	-3
UV / 25 °C / 0 % RH								
0	54 ± 4.8	-	42 ± 7	-	60 ± 5.7	-	5 ± 0.3	-
13±0.5	10 ± 2.7	81	7 ± 3	83	32 ± 4.3	46	4 ± 0.4	22
28±0.5	7 ± 1.4	88	7 ± 1	84	23 ± 2.7	61	3 ± 0.4	24
42±0.5	5 ± 1.2	92	6 ± 1	86	21 ± 3.6	65	3 ± 1.9	40
56±0.5	4 ± 1.1	93	6 ± 0.8	85	17 ± 3.4	71	3 ± 0.5	26
UV /50 °C / 50 % RH								
0	55 ± 8.0	-	41 ± 4	-	55 ± 5.3	-	4 ± 0.3	-
14±0.5	6± 1.4	89	5 ± 0.8	88	27 ± 3.2	51	3 ± 0.1	25
28±0.5	3± 0.9	95	5 ± 1.4	88	16 ± 2.2	71	3 ± 0.2	25
42±0.5	-	-	-	-	12 ± 2.4	78	3 ± 0.1	25
55±0.5	2± 0.4	97	5 ± 1.1	88	9 ± 1.5	84	3 ± 0.2	25

[§] Positive values indicate decrease in tensile strength w.r.t. control sample whereas negative values suggests increase in tensile strength.

[^] Positive values indicate increase in % elongation at break w.r.t. control sample whereas negative values suggest decrease in % elongation at break.

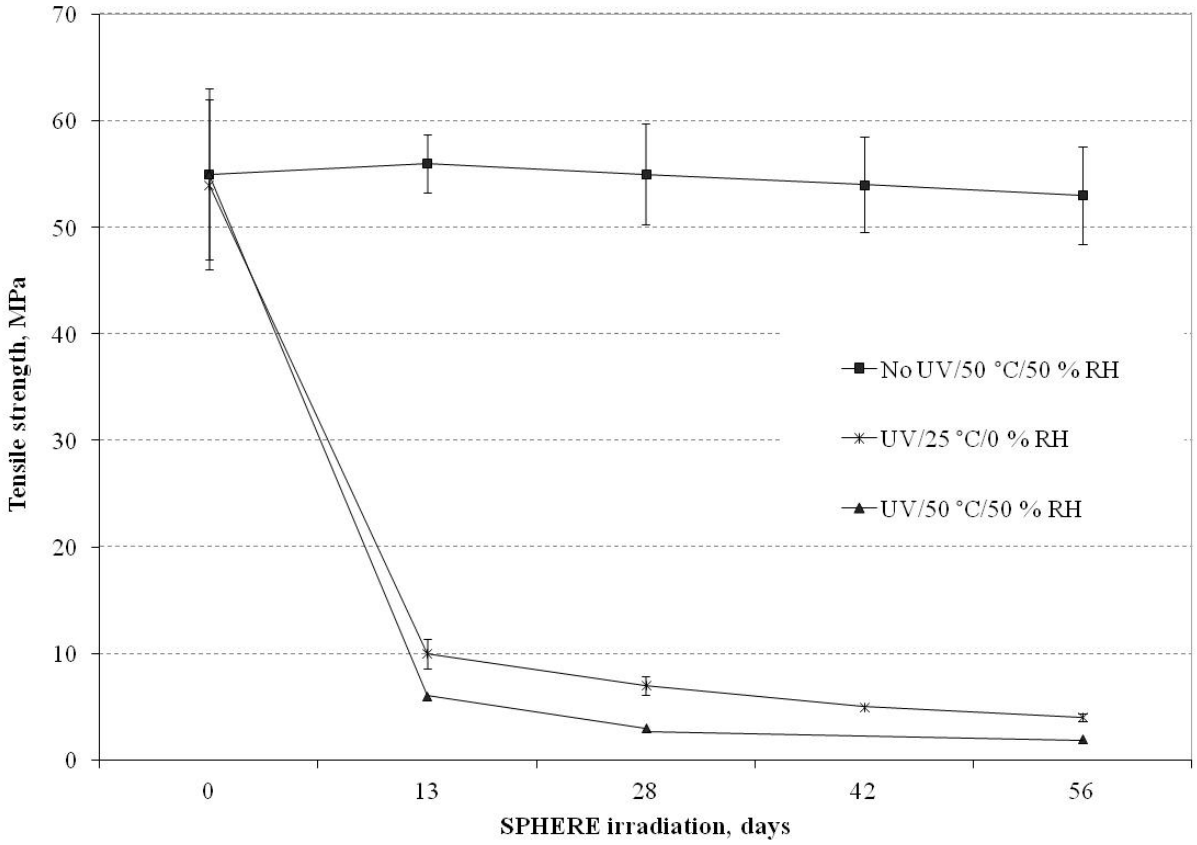
70
60
50
40
30
20
10
0
Tensile strength, MPa
0
13
28
42
56
SPHERE irradiation, days
No UV/50 °C/50 % RH
UV/25 °C/0 % RH
UV/50 °C/50 % RH

(a)

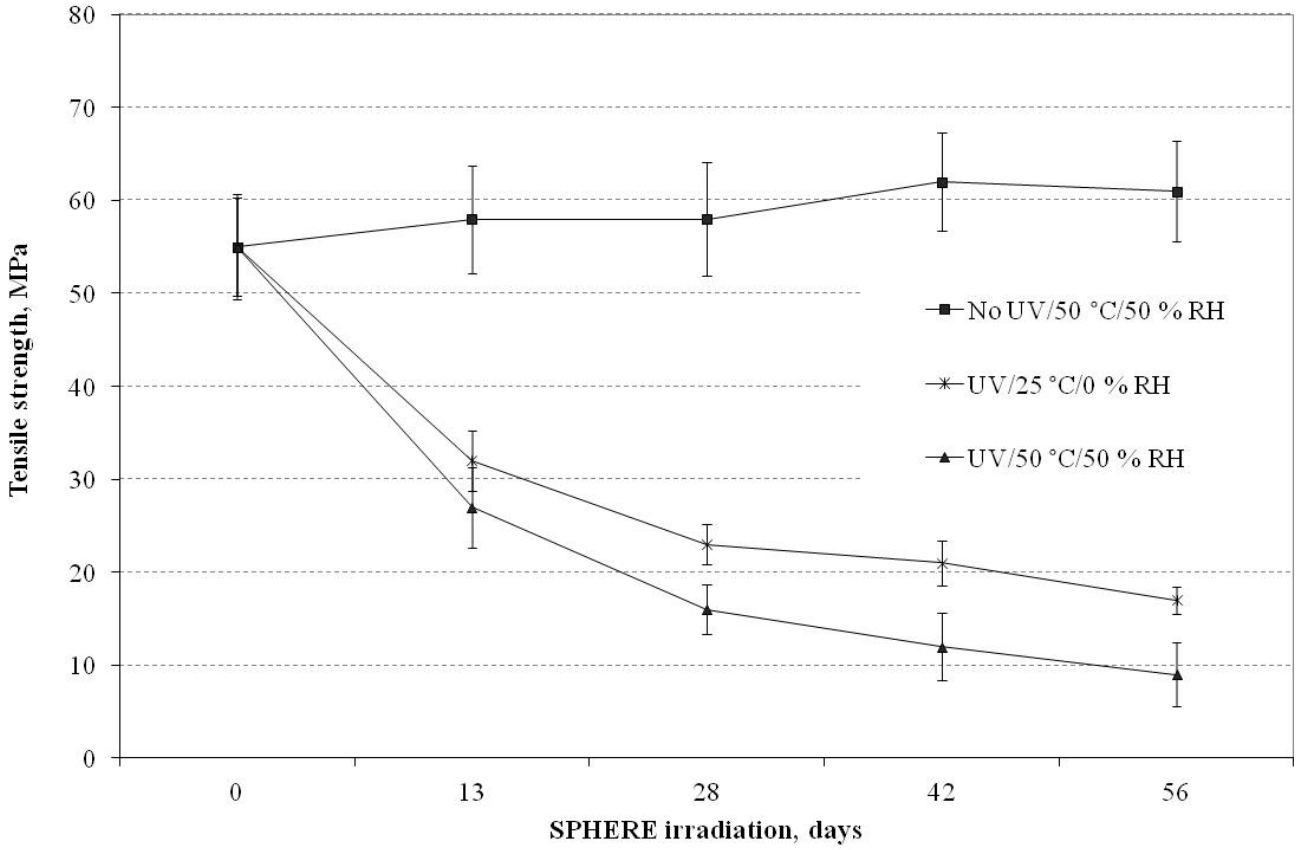

(b)

Figure 3. Deterioration in tensile strength as a function of exposure conditions for (a) NKB and (b) KPB fabrics.

3.3. UV Protection Factor (UPF)

The UV transmittance data for NKB and KPB fabrics is given in Table 4. The UV transmittance of tested fabrics (NKB and KPB) is very low for UV-A (% of UV light transmitted within the wavelength range from 280 nm to 315 nm) or UV-B (% of UV light transmitted within the wavelength range from between 315 nm and 400 nm) and therefore inconclusive. The ultra violet protection factor (UPF) has therefore been calculated, using the methodology described in previous studies [10], to assess and compare the protective performance of fabric samples against UV radiation. Three important factors that are taken into consideration while calculating UPF include: i) spectral transmittance of fabrics, ii) the solar spectral transmittance and iii) the relative erythermal effectiveness. Spectral transmittance of fabric is the proportion of radiant light that passes through the fabric after reflection and absorption by the fabric. The transmittance spectra of fabrics can vary significantly depending on the fibers in fabric composition, structural characteristics of fabric, finishing ancillaries such as optical brightening agents, dyestuff, UV-absorbers etc., and laundering conditions [22]. The higher the transmittance of UV radiation through fabric, the lower the UPF value.

The UPF values for unexposed NKB and KPB fabric samples are 43 and 25 respectively. According to the ASTM D6603 [23] classification system for UV protection of textile materials, NKB exhibits "excellent" UV protection whereas KPB provides reasonable ("very good") protection. While both the fabrics provide sufficient protection to avoid photolytic degradation of underlying layers via solar UV radiation, the proportion of UV radiation passing through KPB fabric is comparatively greater than that passing through NKB. Greater spectral transmittance of KPB may be attributed to lower fabric density (44 warp/inch and 38 weft/inch) compared to that of NKB (50 warp/inch and 42 weft/inch) or higher reflection/absorbance of UV radiation by NKB fabric.

Previous studies on accelerated weathering of NKB and KPB fabrics indicated comparable UPF values for both fabrics after 13 d exposure to UV/50 ^{o}C/ 50 % RH on the NIST SPHERE [10]. However, if we compare the UPF rating (which always has a value which is a multiple of 5) based on UPF classification system described in Table 5, the UPF rating of 40 for NKB is reduced to 20 which is a noticeable reduction from "excellent" protection to "good" protection. The UPF rating for KPB is changed from 25 to 20, which is a marginal change from "very good" to "good" protection. Compared to KPB the UV exposure causes significant change in UV transmittance of NKB. With unaltered fabrics density, greater transmittance of UV exposed NKB suggests greater reflection/absorption of UV radiation due to chemical changes on the surface of NKB fabrics.

Ageing performance profile (APP) in terms of UPF rating for three different exposure conditions have been compared and graphically presented for NKB and KPB fabrics in Figure 4 (a) and (b), respectively. In absence of UV radiation, there is no change in UPF rating of NKB and KPB fabrics suggesting that elevated temperature and increased humidity have no impact on UV transmittance of the fabrics studied. APP profiles for both the fabrics in Figures 4(a) and (b) indicate that UV irradiation at elevated temperature and humidity (UV/50 ^{o}C/50 % RH) and UV irradiation at ambient conditions (UV/25 ^{o}C/0 % RH) has similar impact on UPF rating of fabrics. For both tested fabrics, the 13 d exposure to UV radiation on the NIST SPHERE (which equates to 6.6 years of exposure in natural conditions) has maximum detrimental effect on UV transmittance. Further exposures have no impact on UV transmittance of fabrics.

Table 4. Ultraviolet protection factor (UPF) and the average UV transmittance of NKB and KPB fabrics.

	SPHERE (d)	UPF	$T_{(280-400)}$(%)	$T_{(280-315)}$(%)	$T_{(315-400)}$(%)	$T_{(400-500)}$(%)
NKB	0.0	43	0.12	0.00	0.17	0.10
	No UV / 50 °C / 50 % RH					
	14.0±0.5	41	0.13	0.01	0.09	0.09
	28.0±0.5	43	0.21	0.00	0.15	0.12
	42.0±0.5	44	0.14	0.00	0.10	0.07
	56.0±0.5	42	0.11	0.01	0.09	0.06
	UV / 25 °C / 0 % RH					
	13.5±0.5	25	0.13	0.00	0.20	0.34
	27.7±0.5	18	0.06	0.02	0.14	0.28

	42.0±0.5	18	0.04	0.08	0.16	0.32
	55.8±0.5	18	0.06	0.00	0.16	0.32
KPB	0.0	18	0.06	0.02	0.12	0.22
	No UV / 50 °C / 50 % RH					
	14.0±0.5	24	0.10	0.01	0.13	0.24
	28.0±0.5	22	0.04	0.02	0.05	0.10
	42.0±0.5	22	0.08	0.03	0.10	0.19
	56.0±0.5	24	0.06	0.02	0.08	0.19
	UV / 25 °C / 0 % RH					
	14.0±0.5	18	0.09	0.02	0.12	0.12
	27.8±0.5	18	0.08	0.02	0.11	0.12
	44.0±0.5	18	0.08	0.02	0.10	0.07
	58.4±0.5	18	0.08	0.02	0.10	0.07

Table 5: UPF classification system for textile materials [23]

UPF range	UV radiation Protection category	Effective UV transmission (%)	UPF ratings
15 to 24	Good protection	6.7 to 4.2	15, 20
25 to 39	Very good protection	4.1 to 2.6	25, 30, 35
40 to 50, 50+	Excellent protection	≤ 2.5	40, 45, 50, 50+

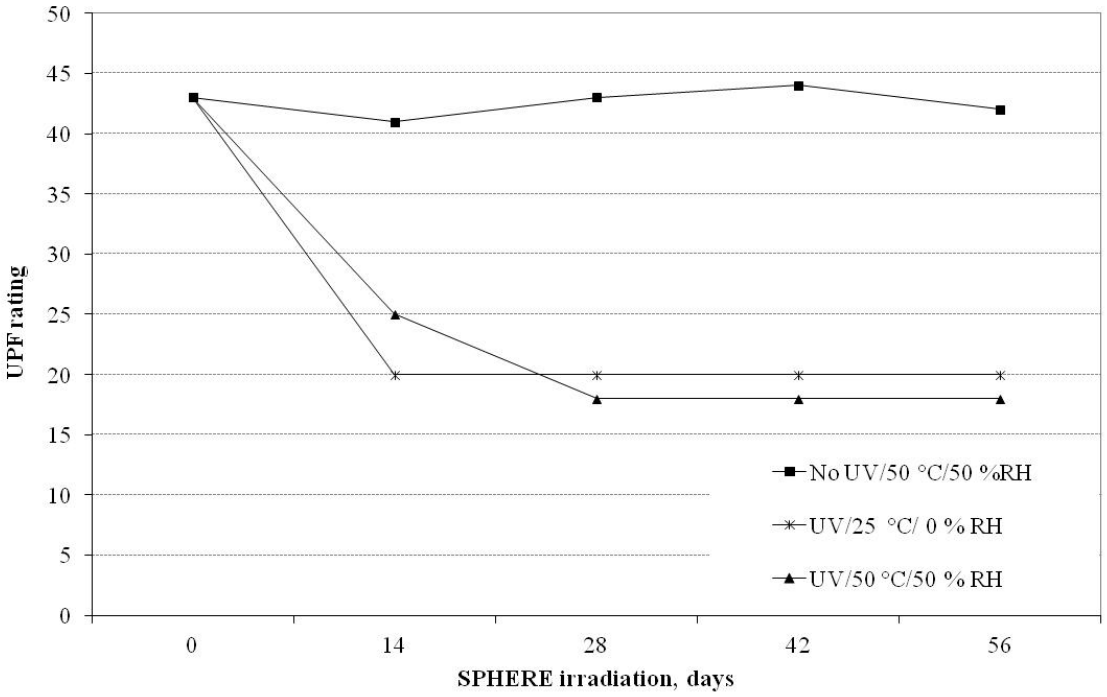

(a)

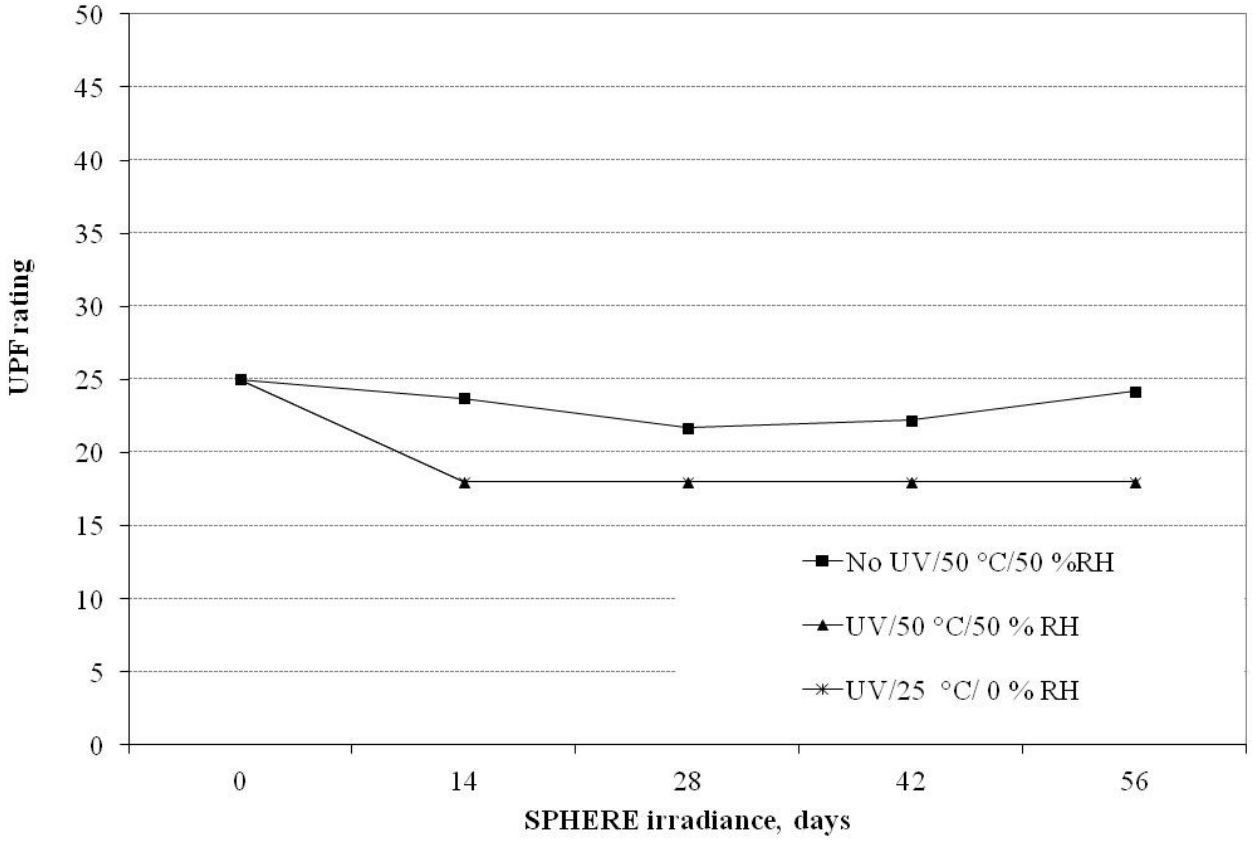

(b)

Figure 4. UPF rating as a function of UV irradiation for: (a) NKB and (b) KPB fabrics.

3.4. Attenuated Total Reflectance Fourier Transform Infrared (ATR-FTIR) Spectroscopy

FTIR spectra interpretation is based on the literature peak assignments of poly(m-phenylene isophthalate), poly(p-phenylene terephthalamide), and polybenzimidazole [24, 25, 26, 27, 28, 29, 30]. The spectra for NKB and KPB fabrics for two different regions are stacked as a function of aging time (Figure 5 and Figure 6, (a) 3550 cm^{-1} to 2950 cm^{-1} and (b) 1825 cm^{-1} to 1625 cm^{-1}). Dash lines are aging at UV/50 ^{o}C/50 % RH, and solid lines at UV/25 ^{o}C/0 % RH, and dotted lines at no UV 50 ^{o}C/50 % RH.

Characteristic peaks of unexposed NKB fabrics can be noted in baseline spectrum shown in Figure 5(a) and (b). The characteristic peaks in Figure 5(a) are 3320 cm^{-1} (N-H stretching of amide) and 3050 cm^{-1} (C-H stretching of aromatic rings), and in Figure 5(b) is 1600 cm^{-1} (stretching of aromatic ring C=C). Other characteristic peaks (not shown here) at 1525 cm^{-1} and 1236 cm^{-1} are assigned to amide II and III, respectively.

The baseline spectrum of unexposed KPB fabric is shown in Figure 6(a) and (b). FTIR spectra of KPB and NKB fabric are similar due to the similar structure of poly(m-phenylene isophthalate) and poly(p-phenylene terephthalamide). The characteristic peaks of polybenzimidazole are 3050 cm^{-1} (aromatic N-H stretching), 1626 cm^{-1} (C=C/C=N

stretching), and 1050 cm^{-1} (benzene ring vibration) have not been identified in Figure 6 as it was difficult to resolve these peaks from the poly(p-phenylene terephthalamide) peaks. Polybenzimidazole is a minor component in the KPB blend and hence also difficult to resolve from the other these peaks. Additionally, a strong heterocyclic peak at 802 cm^{-1} (C-H out-of-plane bending) has not been included in Figure 6.

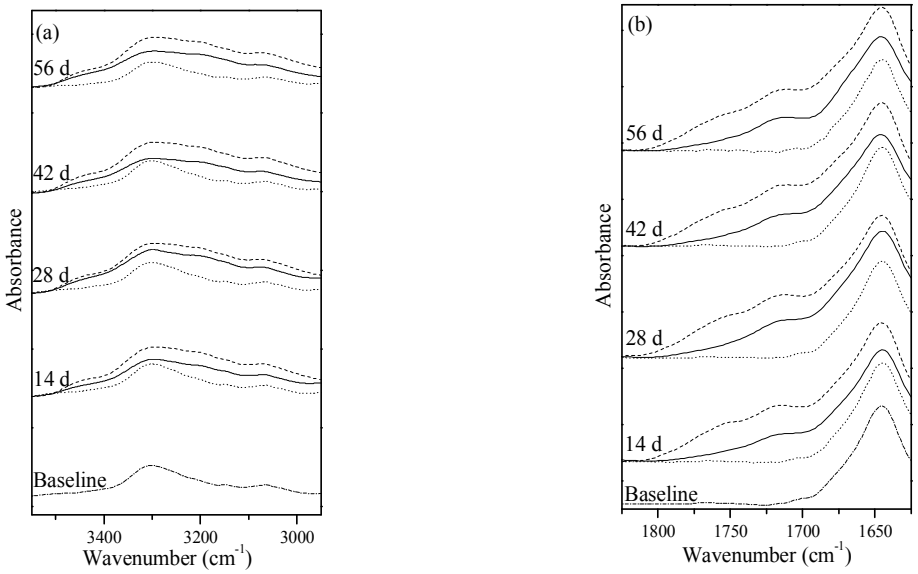

Figure 5. ATR-FTIR spectra of NKB: (a) 3550 cm^{-1} to 2950 cm^{-1} and (b) 1825 cm^{-1} to 1625 cm^{-1} stacked as a functional of aging time. Dash lines are aging at UV/50 ^{o}C/50 % RH, and solid lines at UV/25 ^{o}C/0 % RH, and dotted lines at no UV 50 ^{o}C/50 % RH.

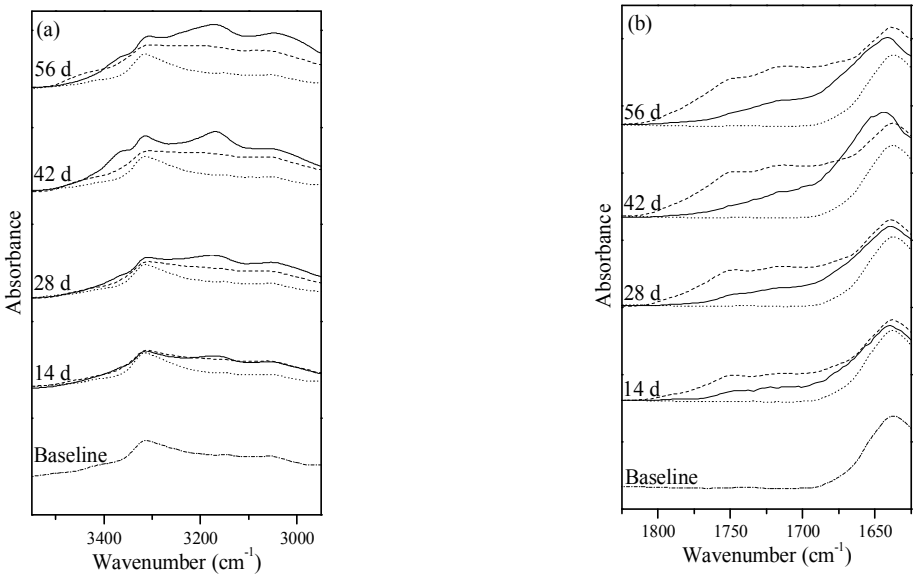

Figure 6. ATR-FTIR spectra of KPB: (a) 3550 cm^{-1} to 2950 cm^{-1} and (b) 1825 cm^{-1} to 1625 cm^{-1} stacked as a function of aging time. Dashed lines represent samples aged at

UV/50 ^{o}C/50 % RH, solid lines samples aged at UV/25 ^{o}C/0 % RH, and dotted lines samples aged with no UV 50 ^{o}C/50 % RH

There was no change in the FTIR spectra of NKB fabrics exposed to elevated temperature and RH with no UV irradiation (no UV/50 ^{o}C/50 % RH), relative to the unexposed NKB baseline (Figure 5(a)). However, exposure to UV irradiation (regardless of temperature and RH) resulted in a change in peak intensity and peak broadening (3320 cm^{-1} ranging from 3500 cm^{-1} to 3000 cm^{-1}). This suggests polymer degradation likely occurred through UV-initiated photolytic oxidation of the amide backbone linkages to form hydroxyl groups. Consistent with this observation is the conversion of the amide peak at 1720 cm^{-1} to a peak consistent with carboxylic acid and/or esters as observed at 1745 cm^{-1} (Figure 5(b)). Additional evidence of amide cleavage is a reduction in peak intensities of Amide I ((1536 cm^{-1}) and Amide II ((1650 cm^{-1}) (not shown here). It should also be noted that UV exposure greater than 14 d appears to cause no further degradation of the NKB fabrics or that the decomposition is below the detection depth of the FTIR analysis.

FTIR spectra of KPB fabrics in Figure 6(a) and (b) show the same trend as NKB except that the magnitude of the peak intensity and peak broadening at 3320 cm^{-1} ranging from 3500 cm^{-1} to 3000 cm^{-1} , which is assigned to formation of O-H group, is greater for KPB fabrics aged at 25 ^{o}C ± 0.1 ^{o}C and 0 % ± 1 % RH in the presence of UV irradiation compared to 50 ^{o}C ± 0.1 ^{o}C and 50 % ± 1 % RH with UV radiation. This can be attributed to the fact that NKB and KPB fabrics have different water-repellent coatings and that this coating is significantly degraded during first 13 d exposure to UV radiation, which in turn affects water absorption properties [10].

4. Summary and Conclusions

The objective of this study was to delineate the individual impacts of UV irradiation, elevated temperature, and moisture on the chemical and mechanical attributes of OS fabrics used in firefighter turnout gear. Results indicate that physical and chemical properties of both the OS fabrics considered in this study remain unaltered when exposed to elevated temperature and moisture (50 °C and 50 % ± 1 % RH). However, exposure of NKB and KPB fabrics to simulated UV light caused rapid and extremely large loss in tear and tensile strength. The aging performance profiles (APP) of both the fabrics were similar in that significant deterioration occurred due to 13 d exposure to UV irradiation. Exposure in excess of 13 d had minimal changes in properties of NKB and KPB fabrics. UV exposure at elevated temperature with higher moisture levels caused slightly greater degradation of constituent fibers due to photo oxidation when compared to UV exposures at ambient temperature and moisture. This study indicates that the deterioration in the physical properties of polyaramids and polybenzimidazole are mainly due to photo-oxidative reactions, which change the chemical composition of the polymeric system. These chemical changes are the result of the breaking of chemical bonds in the polymeric chains and thereby formation of lower molecular weight species. The photochemical reactions are associated with build-up of oxidation reaction products and new polymer

end groups. These changes are known to be responsible for the loss in tensile strength as well as the color change.

Exposure of the fabrics at elevated temperature and humidity, however, has less detrimental effect on UPF rating of fabrics when compared to UV irradiation at ambient conditions, suggesting that if the protective garments are exposed to UV radiation at ambient conditions, then the chances of underlying layers being exposed to UV radiation is greater. It is therefore critical to the service life of firefighters turnout gear that they be stored out of direct sunlight.

Several UV blockers, including organic and inorganic, have recently been developed to improve the UV protective properties of textiles in general. The organic UV blockers absorb UV rays whereas inorganic UV blockers, by virtue of their high refractive indices, operate primarily by reflecting and/or scattering most of the UV rays. The inorganic UV blocking agents are preferred due to their unique features including non-toxicity and chemical stability under both high temperature and UV ray exposure. Titanium dioxide (TiO_2) is a semiconducting, inorganic UV blocking agent and is a very attractive additive for films and fabrics. In general, two main methods used to modify textile materials is the incorporation of additives in the fibers, and application of a functional coating on the fabrics during the finishing process. Currently, we are investigating a novel coating method using a layer-by-layer (LbL) deposition to fabricate nanometer- to micrometer-thick TiO_2 coatings on the high performing fiber fabrics. The LBL coated fabrics will be evaluated for thermal and mechanical properties that are critical to the protective performance of firefighter turnout gear. The performance of LbL coated fabrics exposed to accelerated environmental stressing including UV exposure, laundering , wear and abrasion will also be evaluated.

5. References

[1] NFPA 1851, Standard on Selection, Care and Maintenance of Structural Fire-fighting and Proximity Fire-Fighting Protective Ensembles, National Fire Protection Association, Quincy, Massachusetts, 2008 Edition.

[2] Wall MJ, Frank GC. A study of the spectral distribution of sun-sky and Xenon-arc radiation in relation to the degradation of some textile yarns. Textile Research Journal 1971; 41 (1): 32-38.

[3] Arrieta C, David E, Patricia D and Vu-Khanh T, Thermal aging of a blend of high-performance fibers, Journal of Applied Polymer Science, 115: 3031-3039 (2010)

[4] Blais P, Carlsson DJ, Parnell RD, Wiles DM. High Performance Fibers. Part II: Limitations: Photo-and Thermal Degradation, Canadian Textile Journal 90 (7): 93-96 (1973)

[5] Carlsson DJ, Wiles DM. High performance fibers Part I: Types, properties and applications, Canadian Textile Journal 90 (6): 107-110(1973)

[6] Carlsson DJ, Gan LH, Paranell RD, Wiles DM. The photodegradation of Poly (1,3-Phenylene Isophtalamide) films in air, Journal of Polymer science 1973; Part B 11: 683-688.
[7] Brown JR, Browne NM, Burchill PJ, Egglestone GT. Photochemical ageing of Kevlar 49, Textile Research Journal 1983; 53 (4): 214-219.
[8] Said MA, Dingwall B, Gupta A, Seyam AM, Mock G, Theyson T. Investigation of ultraviolet resistance of high strength fibers 2006; 37: 2052-2058.
[9] Davis A, Howes BV, Howes EA. unpublished research.
[10] Davis R, Chin J, Lin C, Petit S. Accelerated weathering of polyaramid and polybenzimidazole firefighter protective clothing fabrics, Polymer degradation stability 2010; 95: 1642-2654.
[11] NFPA 1971: Standard on Protective Ensembles for Structural Fire Fighting and Proximity Fire Fighting. National Fire Protection Association, Quincy, Massachusetts , 2007 Edition.
[12] Chin J, Byrd E, Embree N, Garver J, Dickens B, Finn T, Martin J. Accelerated UV weathering device based on integrating sphere technology. Review of Scientific Instruments 2004;75: 4951.
[13] ASTM D 5587-Standard test method for the tearing Strength of Fabrics by Trapezoidal method, ASTM, Philadelphia, PA. 2008 Edition.
[14] ASTM D2261 - Standard test method for tearing strength of fabrics by the tongue (single rip) procedure (constant-rate-of-extension tensile testing machine), ASTM, Philadelphia, PA. 2002 Edition. Available from: http://www.astm.org/DATABASE.CART/HISTORICAL/D2261-96R02.htm.
[15] Taylor BN and Kuyatt CE, Guidelines for Evaluating and Expressing the Uncertainty of NIST Measurement Results, NIST Technical Note 1297 1994 Edition (Supersedes 1993 Edition), Gaithersburg, MD, 20878.
[16] Evaluation of measurement data — Guide to the expression of uncertainty in measurement. JCGM 100:2008 http://www.bipm.org/utils/common/documents/jcgm/JCGM_100_2008_E.pdf
[17] ASTM D2256 / D2256M - Standard Test Method for Tensile Properties of Yarns by the Single-Strand Method, ASTM, Philadelphia, PA. 2009 Edition.
[18] Chin J, Byrd E, Embree E, Martin J. Integrating Sphere Sources for UV Exposure: A Novel Approach to the Artificial UV Weathering of Coatings, Plastics and Composites. In: Service Life Prediction: Methodologies and Metrologies. 2002. p. 144-160. Available from: http://www.fire.nist.gov/bfrlpubs/build03/PDF/b03045.pdf.
[19] Dickens B. In: Martin JW, Bauer DR, editors. Service life prediction methodology and metrologies. Washington, DC: American Chemical Society;2001.
[20] Dobb MG, Johnson DJ, and Saville BP. Supramolecular structure of a high-modulus polyaromatic fiber (Kevlar 49), Journal of Polymer Science. Physics, Ed 15. 1977; 2201-2211.
[21] Carlsson D J, Gan LH, And Wiles DM, The photolysis of fully aromatic amides, Canadian Journal of Chemistry 1975; 53: 2337-2344.
[22] Algaba I, Riva A. In vitro measurement of the ultraviolet protection factor of apparel textiles, Coloration Technology 2002; 118: 52-58.

[23] ASTM D6603 - Standard Guide for Labeling of UV-Protective Textiles, ASTM, Philadelphia, PA. 2011 Edition.
[24] Chang Z, Pu H, Wan D. Liu L, Yuan J, Yang Z. Chemical oxidative degradation of Polybenzimidazole in simulated environment of fuel cells. Polymer Degradation and Stability 2009; 94 (8):1206-1212.
[25] Jang MY, Yamazaki Y. Preparation, characterization and proton conductivity of membrane based on zirconium tricarboxybutylphosphonate and polybenzimidazole for fuel cells. Solid State Ionics 2004; 167: 107–112.
[26] Coates J. Interpretation of Infrared Spectra, A Practical Approach. In: Encyclopedia of Analytical Chemistry. Chinchester: John Wiley and Sons Ltd, 2000; pp. 10815-10837.
[27] Tiefenthaler AM, Urban MW. Surface studies of polymer films and fibers by CIRCLE ATR FT-IR. Applied Spectroscopy 1988;42: 163–166.
[28] Deimede V, Voyiatzis GA, Kallitsis JK, Qingfeng L, Bjerrums NJ. Miscibility behavior of polybenzimidazole/sulfonated polysulfone blends for use in fuel cell applications Macromolecules 2000; 33: 7609–7617.
[29] Mosquera ME, Jamond M, Martinez-Alonso A, Tascon JM. Thermal transformations of Kevlar aramid fibers during pyrolysis: infrared and thermal analysis studies. Chemistry of Materials 1994; 6: 1918–1924.
[30] Luo J, Sun Y. Acyclic N-Halamine coated Kevlar fabric materials: preparation and biocidal Functions. Industrial and Engineering Chemistry Research 2008; 47 (15): 5291–5297.